Full-dimensional quantum dynamics calculations of H_2–H_2 collisions

N. Balakrishnan,[1,a)] G. Quéméner,[2] R. C. Forrey,[3] R. J. Hinde,[4] and P. C. Stancil[5]
[1]*Department of Chemistry, University of Nevada Las Vegas, Las Vegas, Nevada 89154, USA*
[2]*JILA, University of Colorado, Boulder, Colorado 80309-0440, USA*
[3]*Department of Physics, Penn State University, Berks Campus, Reading, Pennsylvania 19610-6009, USA*
[4]*Department of Chemistry, University of Tennessee, Knoxville, Tennessee 37996, USA*
[5]*Department of Physics and Astronomy and the Center for Simulational Physics, University of Georgia, Athens, Georgia 30602, USA*

(Received 16 August 2010; accepted 17 October 2010; published online 3 January 2011)

We report quantum dynamics calculations of rotational and vibrational energy transfer in collisions between two *para*-H_2 molecules over collision energies spanning from the ultracold limit to thermal energies. Results obtained using a recent full-dimensional H_2–H_2 potential energy surface (PES) developed by Hinde [J. Chem. Phys. **128**, 154308 (2008)] are compared with those derived from the Boothroyd, Martin, Keogh, and Peterson (BMKP) PES [J. Chem. Phys. **116**, 666 (2002)]. For vibrational relaxation of $H_2(v = 1, j = 0)$ by collisions with $H_2(v = 0, j = 0)$ as well as rotational excitations in collisions between ground state H_2 molecules, the PES of Hinde is found to yield results in better agreement with available experimental data. A highly efficient near-resonant energy transfer mechanism that conserves internal rotational angular momentum and was identified in our previous study of the H_2–H_2 system [Phys. Rev. A **77**, 030704(R) (2008)] using the BMKP PES is also found to be reproduced by the Hinde PES, demonstrating that the process is largely insensitive to the details of the PES. In the absence of the near-resonance mechanism, vibrational relaxation is driven by the anisotropy of the potential energy surface. Based on a comparison of results obtained using the Hinde and BMKP PESs with available experimental data, it appears that the Hinde PES provides a more accurate description of rotational and vibrational transitions in H_2–H_2 collisions, at least for vibrational quantum numbers $v \leq 1$. © *2011 American Institute of Physics*. [doi:10.1063/1.3511699]

I. INTRODUCTION

Recent advances in creating dense samples of cold and ultracold molecules have engendered considerable interest in atom–molecule and molecule–molecule interactions at ultracold temperatures. Initial studies of ultracold molecule collisions were largely centered around rotational and vibrational relaxation in diatomic molecules induced by collisions with rare gas atoms.[1–8] These studies demonstrated that rotational and vibrational relaxation of molecules at ultracold temperatures obey quantum mechanical threshold behavior and the corresponding rate coefficients attain finite values in the limit of zero temperature, in accordance with Wigner's law.[9] The limiting values of the vibrational relaxation rate coefficients were found to be strongly sensitive to the initial rovibrational levels of the molecule.[1] Subsequent studies of barrierless alkali- and nonalkali-metal atom–dimer systems indicated that the zero-temperature inelastic and reactive rate coefficients can attain large values, on the order of 10^{-11}–10^{-10} cm^3 molecule^{-1} s^{-1} (Refs. 10–15) and that the rate coefficients are less sensitive to the initial vibrational level of the molecule.[16] Calculations of the $F + H_2$ reaction, which has an energy barrier of about 500 K, indicated that the reaction may occur with a rate coefficient of about 10^{-12} cm^3 molecule^{-1} s^{-1} at ultralow temperatures.[17] Since the reaction occurs primarily through tunneling at low temperatures, this has prompted several subsequent studies of tunneling dominated reactions at ultracold temperatures.[18–27] These studies revealed that the van der Waals interaction potential in the incident channel may play a key role in the reactive outcome and that in reactions involving vibrationally excited molecules the reactive pathway may compete or dominate over nonreactive vibrational quenching.[21,23,24,27] Because perturbations induced by an external electric or magnetic field are significant at sub-Kelvin temperatures, external field (both electric and magnetic) control of molecular collisions and chemical reactions at ultracold temperatures has gained considerable theoretical attention[2,28–33] and important progress has been made at the experimental front recently.[34,35]

While most collisional studies of ultracold molecules have focused on atom–diatom systems, molecule–molecule collisions have received much less attention. At high densities of trapped molecules, molecule–molecule collisions become more important than atom–dimer collisions and they become the main source of trap loss. The primary difficulty in theoretical studies of molecule–molecule collisions is the increase in dimensionality in going from triatomic to tetra-atomic systems. For this reason, initial collisional studies by Forrey[36] and Lee *et al.*[37] have focused on the H_2–H_2 system by treating the H_2 molecules as rigid rotors. Flower and Roueff [38,39] reported quantum calculations of rovibrational transition in H_2–H_2 collisions by treating one of the H_2 molecules as a rigid rotor. Recently, Quéméner *et al.*[40,41] have extended the formalism to include the fully six-dimensional configuration space, without employing the angular momentum decoupling

[a)]Author to whom correspondence should be addressed. Electronic mail: naduvala@unlv.nevada.edu.

approximations used in previous full-dimensional studies of the H_2–H_2 system at higher temperatures.[42–44] One of the key findings of Quéméner *et al.*[40] is that for certain combinations of initial rovibrational levels of the two molecules, quasiresonant transitions at ultracold temperatures can occur through a highly efficient pathway that conserves the total rotational angular momentum of the two molecules and nearly conserves the internal energy. Time-dependent quantum calculations of H_2–H_2 collisions without decoupling approximations have also been reported but these methods are generally better suited for higher temperatures.[45,46] Here we focus on molecule–molecule collisions taking the H_2–H_2 system as an illustrative example.

The H_2–H_2 system has long been considered as a benchmark candidate for quantum dynamics studies of molecule–molecule collisions. Being the most abundant molecular species in the interstellar medium, rotational and vibrational transitions in collisions between H_2 molecules have been topics of considerable interest.[38,39,47–49] A number of potential energy surfaces for the H_4 system have been reported in the literature and dynamics calculations using quasiclassical trajectory, semiclassical, and quantum mechanical methods have been performed by different investigators. In particular, a six-dimensional potential energy surface (PES) developed by Boothroyd, Martin, Keogh, and Peterson (BMKP) (Ref. 50) has been adopted in a number of quantum dynamics calculations of the H_2–H_2 system. However, the accuracy of this potential has come under scrutiny because it yields values for rotational excitation rate coefficients in collisions of two ground state *para*-H_2 molecules that are too low[37] or values for vibrational de-excitation cross sections in $H_2(v = 1, j = 0) + H_2(v = 0, j = 0)$ collisions that are too large.[41,42] The large values for the vibrational relaxation cross sections were attributed to high-order anisotropies in the angular expansion of the interaction potential.[42] In contrast, the PES developed by Diep and Johnson (DJ) (Ref. 51) was found to yield $0 \rightarrow 2$ rotational excitation cross sections in collisions of rotationally ground state *para*-H_2 molecules in close agreement with experimental results.[52] However, this surface is restricted to rigid rotor collisions and it cannot describe vibrational transitions. A more accurate potential for the H_2–H_2 system within the rigid rotor model and using very large orbital basis sets (up to augmented quintuple zeta size supplemented with bond functions) has also been reported by Patkowski *et al.*[53] Recently, Hinde[54] reported a full-dimensional PES for the H_2–H_2 system that includes an accurate description of the van der Waals interaction region. This surface is primarily based on high quality *ab initio* data but includes two empirical parameters to accurately reproduce bound and quasibound energy levels of H_2-D_2 and D_2–D_2 van der Waals complexes.[54]

Here we report full-dimensional quantum calculations of rovibrational transitions in the H_2–H_2 system using the PES of Hinde[54] and compare the results with those obtained using the BMKP surface and its less anisotropic BMKPE version.[42] The near-resonant rotation–vibration energy transfer identified by Quéméner *et al.*[40] using the BMKP PES is also equally well reproduced by the PES of Hinde, demonstrating that the mechanism is largely insensitive to the fine details of the PES. Temperature dependent rate coefficients for vibrational relaxation of $H_2(v = 1)$ induced by $H_2(v = 0)$ collisions derived from the Hinde potential are found to be in good agreement with the experiment.

II. METHODOLOGY

The quantum dynamics formalism used is the same as that employed in our two previous articles[40,41] and only a brief description of the methodology is given here. For details of the theoretical formalism we refer to Ref. 41 We use a time-independent quantum formalism based on Jacobi coordinates to describe the scattering of two $^1\Sigma$ diatomic molecules without employing any angular momentum decoupling approximations. The methodology has been described by Takayanagi,[55] Green,[56] Alexander and DePristo,[57] and Zarur and Rabitz,[58] using the close-coupling formalism of Arthurs and Dalgarno[59] and it has been implemented in the TwoBC – Quantum Scattering Code.[60] The notation $(v_1\, j_1\, v_2 j_2)$, referred to as a combined molecular state (CMS), is used to describe the $H_2(v = v_1, j = j_1) + H_2(v = v_2, j = j_2)$ collision system where v_i and j_i are the vibrational and rotational quantum numbers.

The close-coupling method uses an expansion of the angular dependence of the interaction potential in terms of a product of spherical harmonics,[41]

$$U(\vec{r}_1, \vec{r}_2, \vec{R}) = \sum_{\lambda} A_\lambda(r_1, r_2, R) Y_\lambda(\hat{r}_1, \hat{r}_2, \hat{R}), \tag{1}$$

where $\vec{r}_1$ and $\vec{r}_2$ represent the vectors joining the two atoms of the two H_2 molecules and $\vec{R}$ denotes the vector joining the centers of mass of the two molecules. The functions Y_λ are given by

$$Y_\lambda(\hat{r}_1, \hat{r}_2, \hat{R}) = \sum_m \langle \lambda_1 m_1 \lambda_2 m_2 | \lambda_{12} m_{12} \rangle \times Y_{\lambda_1 m_1}(\hat{r}_1) Y_{\lambda_2 m_2}(\hat{r}_2) Y^*_{\lambda_{12} m_{12}}(\hat{R}), \tag{2}$$

where $\lambda \equiv \lambda_1 \lambda_2 \lambda_{12}$ and $m \equiv m_1 m_2 m_{12}$. The notation $\langle \lambda_1 m_1 \lambda_2 m_2 | \lambda_{12} m_{12} \rangle$ refers to a Clebsch–Gordan coefficient. For each value of the center-of-mass distance, R, the Schrödinger equation is solved by propagating the log-derivative matrix, following methods developed by Johnson[61] and Manolopoulos.[62] This yields the scattering matrix from which state-to-state cross sections for transitions from an initial CMS $(v_1\, j_1\, v_2 j_2)$ to final states $(v_1'\, j_1'\, v_2'\, j_2')$ are calculated.

In defining state-to-state cross sections, distinction must be made between collisions involving distinguishable and indistinguishable molecules. For indistinguishable molecules as in the present case, the state-to-state cross sections must be statistically weighted by the two molecular spin exchange-permutation symmetry components,

$$\sigma_{v_1 j_1 v_2 j_2 \rightarrow v_1' j_1' v_2' j_2'}(E_c) = W^+ \sigma^{\varepsilon_P = +1} + W^- \sigma^{\varepsilon_P = -1} \tag{3}$$

with

$$\sigma^{\varepsilon_P} = \frac{\pi(1+\delta_{v_1v_2}\delta_{j_1j_2})(1+\delta_{v_1'v_2'}\delta_{j_1'j_2'})}{(2j_1+1)(2j_2+1)k^2} \times \sum_{j_{12}j_{12}'ll'J\varepsilon_I}^{*} (2J+1)\left|\delta_{v_1j_1v_2j_2,v_1'j_1'v_2'j_2'} - S^{Jj_{12}j_{12}'\varepsilon_I\epsilon_P}_{v_1j_1v_2j_2,v_1'j_1'v_2'j_2'}(E_c)\right|^2, \quad (4)$$

where k is the wave vector associated with the collision energy E_c, l is the orbital angular momentum quantum number, j_{12} is the total rotational angular momentum quantum number, J is the total angular momentum quantum number, ε_I is the eigenvalue of the spatial inversion operator, and S is an element of the scattering matrix. The superscript over the sum indicates that the summation is over states that are "well ordered," which in the present case includes $v_1 > v_2$, and if $v_1 = v_2$, $j_1 \geq j_2$. In collisions of *para*-H_2 molecules for which nuclear spin $I = 0$, $W^+ = 1$, $W^- = 0$, and only the $\varepsilon_P = +1$ symmetry is needed in the close-coupling calculation. For collisions involving *ortho*-H_2 molecules (nuclear spin $I = 1$), $W^+ = 2/3$, $W^- = 1/3$, and both symmetries $\varepsilon_P = \pm 1$ are required.

The total inelastic cross section is given by the sum of all inelastic state-to-state cross sections. Thermal averaging the cross sections over a Maxwell–Boltzmann distribution of collision energies yields rate coefficients as a function of the temperature.

III. RESULTS AND DISCUSSION

A. Vibrational relaxation

First we discuss some aspects of convergence of the state-to-state cross sections. Convergence has to be sought with respect to the rotational and vibrational levels of the two molecules included in the close-coupling scheme as well as the number of anisotropic terms included in the expansion of the angular part of the interaction potential [Eq. (1)]. These issues have been discussed in detail in our previous studies[40,41] using the BMKP PES. Here we focus mainly on the convergence with respect to the number of terms included in the angular expansion of the interaction potential. This is shown in Fig. 1 for $H_2(v = 1, j = 0) + H_2(v = 0, j = 0) \rightarrow H_2(v = 0, j) + H_2(v = 0, j)$ collisions for both the Hinde and BMKP PESs, at a collision energy of 10^{-3} K. While the Hinde PES yields identical results for $\lambda_1 = \lambda_2 = 2$ and 4, the BMKP PES requires terms up to 8 for these quantities.[41] In our previous paper we have shown that $\lambda_1 = \lambda_2 = 8$ and 10 yield similar results on the BMKP PES.[41] Thus, the BMKP PES is much more anisotropic than the Hinde PES for the H_2–H_2 system. It is this high anisotropy that leads to much larger values of vibrational relaxation rate coefficients for the BMKP PES compared to experimental data.[42] For the rest of the calculations, we employ $\lambda_1 = \lambda_2 = 2$ for the Hinde PES.

We have also carried out extensive convergence tests with respect to the rovibrational levels of the two molecules included in the calculations. For calculations involving vibrationally excited molecules we included vibrational levels

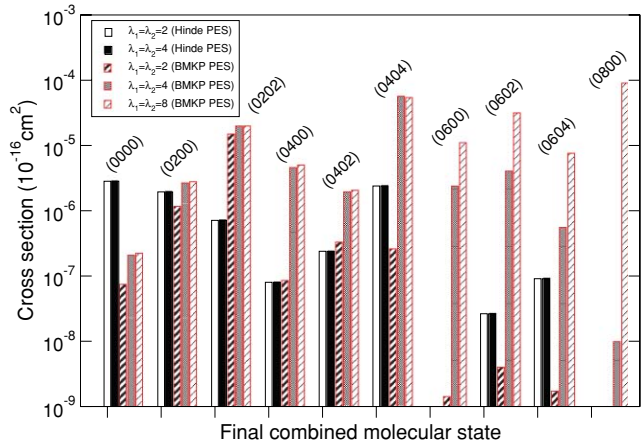

FIG. 1. Convergence of the state-to-state cross sections for $H_2(v = 1, j = 0) + H_2(v = 0, j = 0)$ collisions with respect to the number of terms in the angular expansion of the interaction potential for a collision energy of 10^{-3} K. The black distribution corresponds to the Hinde PES and the red distribution corresponds to the BMKP PES (taken from Ref. 41).

$v = 0$ and $v = 1$ with rotational levels $j = 0 - 10$ in $v = 0$ and $j = 0 - 6$ in $v = 1$. The H_2 potential of Schwenke[67] is used to calculate energy levels and vibrational wave functions of the H_2 molecule. To make the calculations affordable an energy cut-off of 14 000 cm^{-1} was imposed and all CMSs with energy lower than the cut-off energy were included in the calculations. This led to a total of 42 CMSs. A sufficient number of total angular momentum partial waves have been included in the calculations to secure convergence of the computed cross sections. The range in J varied from 0 to 100 with the maximum depending on the collision energy. For $J > 15$ a total of 1378 channels are present which makes the calculations very computer intensive for higher energies.

In Fig. 2, we present total inelastic cross sections for different initial states of the molecules computed using the BMKP and Hinde PESs for collision energies ranging from 10^{-6} to 100 K. Three different combinations of initial states

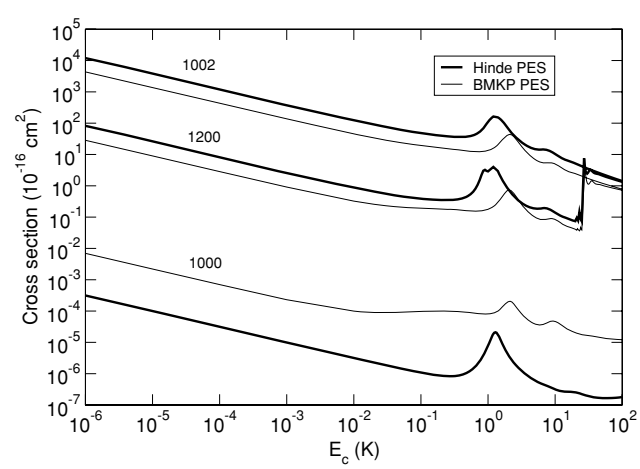

FIG. 2. Vibrational relaxation cross sections as a function of the collision energy for $H_2(v = 1, j = 0) + H_2(v = 0, j = 0)$, $H_2(v = 1, j = 2) + H_2(v = 0, j = 0)$, and $H_2(v = 1, j = 0) + H_2(v = 0, j = 2)$ collisions. The bold line corresponds to the Hinde PES while the thin line corresponds to the BMKP PES (taken from Ref. 41).

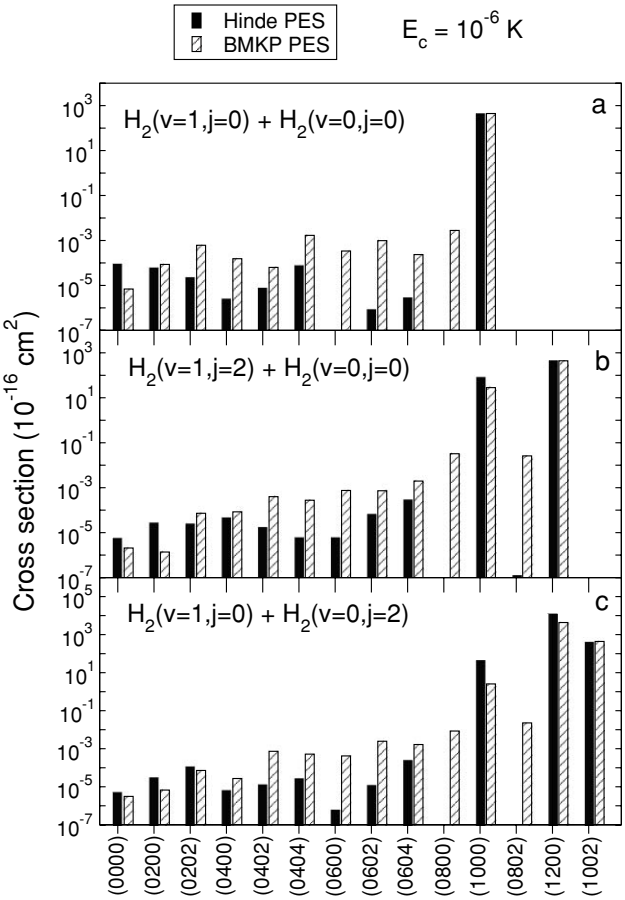

FIG. 3. State-to-state cross sections for $H_2(v = 1, j = 0) + H_2(v = 0, j = 0)$, $H_2(v = 1, j = 2) + H_2(v = 0, j = 0)$, and $H_2(v = 1, j = 0) + H_2(v = 0, j = 2)$ collisions at an incident kinetic energy of 10^{-6} K. The black distribution corresponds to the Hinde PES while the white and dashed distribution corresponds to the BMKP PES (taken from Ref. 41).

are considered here with one molecule in the $v = 1$ vibrational level and the other molecule in the vibrationally ground state. The initial rotational levels of the two molecules are different in the three cases. In the CMS notation the three initial states are (i) (1000), (ii) (1200), and (iii) (1002). As Fig. 2 illustrates the results depend strongly on the initial rotational and vibrational levels of the two molecules as well as the choice of the PES. Two main features can be noted in Fig. 2: (a) the cross sections are widely different for the three initial states and (b) the BMKP and Hinde PESs yield results that differ by more than an order of magnitude for the CMS (1000) but the agreement between the two PESs is improved for the other two cases. In our previous work using the BMKP PES we have shown that the large values of relaxation cross sections for the (1002) initial state is due to a near-resonant transition that conserves the total rotational angular momentum of the two molecules. In the discussions below we show that the same argument applies for the results obtained using the Hinde PES and that the near-resonant transition is largely independent of the details of the PES. By examining the state-to-state cross sections we will also explain the relative magnitudes of the cross sections for the three initial states obtained using the two PESs.

Figures 3(a)–3(c) show state-to-state cross sections for the three initial states obtained from the two PESs at a collision energy of 10^{-6} K. Each of the open channels is labeled by a CMS index and is shown in the order of increasing total internal energy. It is seen that the final state distributions are quite different for the three cases. The final rotational population is dictated by a competition between internal energy conservation and total rotational angular momentum conservation.[40] Generally, when the internal energy is nearly conserved in the vibrational relaxation process, transition occurs to an excited rotational level that lies just below the initial channel (or just above for excitation collisions). In this case, the kinetic energy in the incident and outgoing channel will be nearly the same leading to similar radial wavefunctions in the two channels resulting in strong radial overlaps. If the magnitude of the change in internal energy is denoted by $\Delta\varepsilon = |\varepsilon^f - \varepsilon^i|$, then $\Delta\varepsilon$ has to be the smallest for the most favorable radial overlaps. Large values of $\Delta\varepsilon$ will lead to dissimilar radial wavefunctions in the two channels, one with a low oscillatory behavior and the other with a high oscillatory behavior resulting in small values of the inelastic quenching cross sections. The total angular momentum J is conserved before and after the collision such that $\Delta J = \Delta j_{12} + \Delta l = 0$ where Δj_{12} and Δl denote, respectively, the difference in the total rotational angular momentum quantum numbers and orbital angular momentum quantum numbers before and after the collision. Transitions which have small internal energy and internal angular momentum gaps are generally very efficient and may be described by energy and angular momentum gap laws.[63] State selectivity is enhanced even more as the collision energy is decreased. At ultralow energies, only the s-wave ($l = 0$) is important for the incident channel and couplings between CMSs with $\Delta j_{12} = 0$ (same initial and final total rotational angular momentum) will dominate. In this case, conservation of the total angular momentum requires that $\Delta l = 0$, leading to an outgoing channel with no centrifugal barrier. For transitions with $\Delta j_{12} \neq 0$, the outgoing channel will experience a centrifugal barrier corresponding to $l = \Delta j_{12}$ with diminished coupling between rotational levels. In the ideal case, if both conditions are simultaneously satisfied ($\Delta\varepsilon \approx 0$ and $\Delta j_{12} = 0$), one can expect a highly efficient near-resonant transition between the initial and a final CMS.

For case (a) shown in the top panel of Fig. 3, both conditions cannot be fulfilled simultaneously. While the transition (1000) → (0000) satisfies $\Delta j_{12} = 0$, it has the largest energy gap $\Delta\varepsilon$. On the other hand, the (1000) → (0800) transition has the smallest energy gap but also has $l = \Delta j_{12} = 8$. Thus the final-state distribution is dictated by a compromise between these two conditions and consequently no single final state is preferentially populated. For case (b) (middle panel of Fig. 3), the two criteria are not satisfied either, but compared to the preceding case, the transition (1200) → (1000) is more favorable than the others because it leads to the smallest energy and angular momentum gaps. This transition involves (for s-wave scattering in the incident channel) $\Delta j_{12} = -2$, $\Delta l = 2$, and relatively small $\Delta\varepsilon$. For case (c) (bottom panel of Fig. 3), both criteria are simultaneously satisfied for the transition (1002) → (1200) and it becomes the dominant transition. This involves $\Delta j_{12} = \Delta l = 0$ and $\Delta\varepsilon = 25.45$ K which

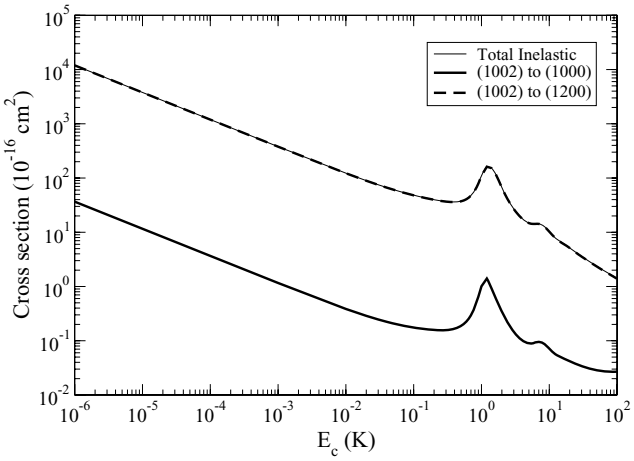

FIG. 4. Comparison of total inelastic cross sections for $H_2(v = 1, j = 0) + H_2(v = 0, j = 2)$ collisions with state-to-state cross sections corresponding to the near-resonant (1200) and the next leading (1000) final states as a function of the collision energy.

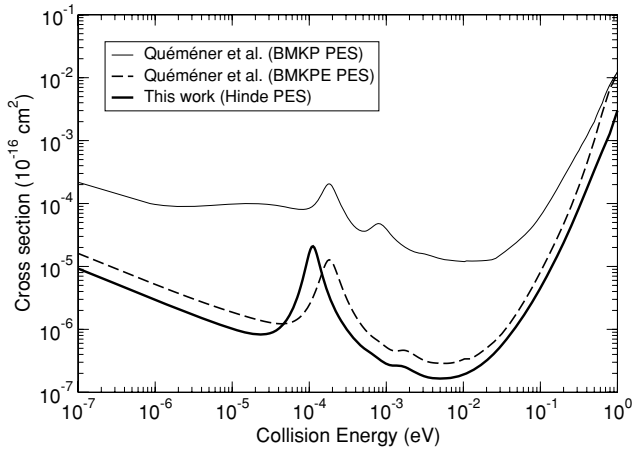

FIG. 5. Inelastic cross sections for $H_2(v = 1, j = 0) + H_2(v = 0, j = 0) \rightarrow H_2(v = 0) + H_2(v = 0)$ collisions from ultracold to thermal energies. The bold line corresponds to the Hinde PES while the thin solid and dashed lines correspond, respectively, to the BMKP and BMKPE PESs (taken from Ref. 41).

is the smallest possible energy defect. For higher energies, the orbital angular momentum increases and may change during the collision. The near resonant (1002) → (1200) transition persists and at energies above 25.45 K, the reverse transition is open with approximately the same efficiency (see Fig. 2).

To illustrate the efficiency of near-resonant transitions when the energy and angular momentum gaps are simultaneously satisfied we compare in Fig. 4 the total inelastic cross section for the (1002) initial state with the near-resonant (1200) and the next dominant (1000) final states. For clarity, only results obtained using the Hinde potential are included. It is seen that the total inelastic cross section is almost completely dominated (more than 99%) by the near-resonant transition over the entire energy range. Thus, the near-resonant process is not just restricted to ultralow energies but occurs over a broad spectrum of energies where a range of total angular momentum quantum numbers ($J = 0$–10 in this case) contribute to the cross section.

The large discrepancy between the results on the two PESs for the CMS (1000) can also be explained based on the state-to-state cross sections. Since the near-resonant condition is not satisfied in this case, the final-state distribution is largely determined by the anisotropy of the PES. Since inclusion of high-order anisotropic terms in the angular dependence of the interaction potential is important for yielding converged results on the BMKP PES (see Fig. 1), the state-to-state cross sections are dominated by contributions from high anisotropic terms. Since anisotropic terms beyond $\lambda_1 = \lambda_2 = 2$ are not important for the Hinde PES, transitions to final CMS (0600), (0602), (0604), and (0800) are significantly suppressed for the Hinde PES compared to the BMKP surface. For the other two initial states, energy and angular momentum conservation factors dictate the overall quenching cross section as explained above.

In an earlier quantum mechanical investigation using the coupled-states approximation, Pogrebyna and Clary[42] indicated that the high anisotropic terms in the angular expansion of the BMKP PES were primarily responsible for the large values of vibrational relaxation cross sections in collisions of $H_2(v = 1, j = 0)$ with $H_2(v = 0, j = 0)$ evaluated using this potential. Calculations using a less anisotropic version of the potential, referred to as the BMKPE potential, in which terms beyond $\lambda_1 = \lambda_2 = 2$ are omitted from Eq. (1) yielded vibrational relaxation cross sections that are in better agreement with experimental data. While the BMKPE potential excludes high-order angular anisotropic terms it incorporates the most important lowest-order quadrupole–quadrupole and dispersion interactions.

In Fig. 5 we present a comparison of vibrational relaxation cross sections for $H_2(v = 1, j = 0) + H_2(v = 0, j = 0)$ collisions obtained from the Hinde PES and the BMKP and BMKPE surfaces. It is seen that compared to the results on the Hinde PES the BMKP surface yields relaxation cross sections that are about an order of magnitude larger at energies below 0.1 eV. Interestingly, the BMKPE and Hinde PESs yield results within a factor of two with the Hinde potential yielding lower values, except in the vicinity of a shape resonance at 10^{-4} eV. This indicates that the less anisotropic BMKPE PES may be more suitable for describing vibrational relaxation than the original BMKP PES. Figure 6 provides a comparison of the vibrational relaxation rate coefficients from the three PESs with available experimental data. The Hinde potential yields rate coefficients in closer agreement with experiment than the BMKP and BMKPE potentials. The agreement is particularly good for temperatures below 200 K. However, results on the Hinde potential underestimate the experimental data at temperatures above 300 K. This could be because the experimental results may include a thermal population of rotational levels in $v = 1$ while our calculation is restricted to the $j = 0$ level of the vibrationally excited molecule. In constrast, the BMKP results are about an order of magnitude larger than the experimental data for temperatures below 300 K. We note that the less anisotropic BMKPE PES yields rate coefficients in much better agreement with experiment than the full anisotropic BMKP PES.

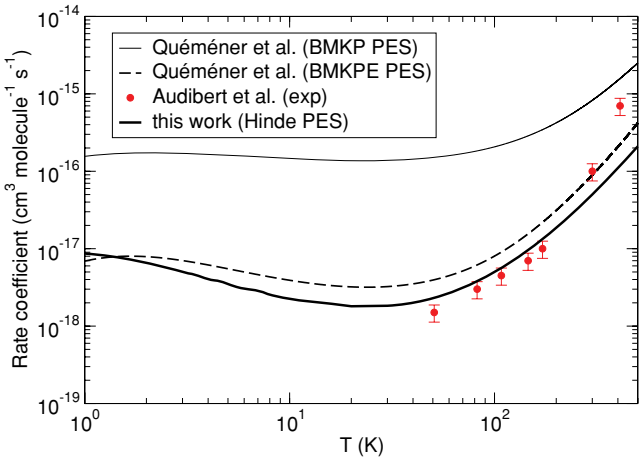

FIG. 6. Rate coefficient for vibrational relaxation of $H_2(v = 1, j = 0)$ in collisions with $H_2(v = 0, j = 0)$ as a function of the temperature. Results on the Hinde PES are shown by the bold curve while that on the BMKP and BMKPE PESs are shown, respectively, by the thin solid and dashed curves (taken from Ref. 41). Experimental results of Audibert *et al.* (Ref. 64) are shown by filled circles with error bars.

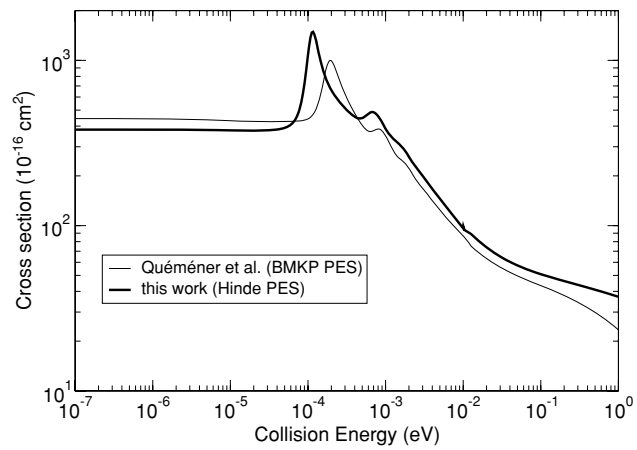

FIG. 8. Elastic cross section for $H_2(v = 1, j = 0) + H_2(v = 0, j = 0)$ collisions from ultracold to thermal energies. The thick curve corresponds to the Hinde PES while the thin curve corresponds to the BMKP PES (taken from Ref. 41).

The large values of vibrational relaxation cross sections and rate coefficients from the BMKP PES compared to the Hinde potential can easily be understood from the state-to-state cross sections shown in the upper panel of Fig. 3 and discussion pertaining to it. Since low temperature cross sections are generally strongly influenced by van der Waals forces, it would also be useful to examine the interaction energies in the van der Waals region for the different PESs. This is shown in Fig. 7 for BMKP, BMKPE, Hinde, and DJ PESs as a function of the center-of-mass distance between the two H_2 molecules for orientation angles $\theta_1 = \theta_2 = 90^\circ$ and $\phi = 0^\circ$. The H–H distance of the two H_2 molecules is fixed at the vibrationally averaged rigid rotor value of 1.449 a.u. (1 a.u. = 0.529 177 2 Å). It is seen that the DJ and Hinde PESs depict similar energy dependence and comparable van der Waals well depths while the BMKP and BMKPE PESs display slightly different energy dependence and deeper van der Waals wells. In particular, the BMKP/BMKPE PESs are characterized by a broader van der Waals region compared to the Hinde and DJ potentials. The rather limited accuracy of the BMKP PES near the van der Waals well has been pointed out in recent works of Hinde[54] and Patkowski *et al.*[53] Indeed, due to the low accuracy of *ab initio* points in the van der Waals region, Boothroyd *et al.*[50] used the rigid rotor potential of Schafer and Kohler[66] in fitting the van der Waals part of the BMKP PES. The van der Waals well of the BMKPE potential is slightly less deeper than the BMKP potential and it is in better agreement with the Hinde potential near the van der Waals minimum. This might explain the overall good agreement between rate coefficients from BMKPE and Hinde PESs. The BMKP and BMKPE potentials are very similar for $R > 8$ a.u. because high anisotropic terms of the interaction potential do not contribute at large intermolecular separations. Thus, the difference between the BMKP and BMKPE potentials appears to be mainly centered around the van der Waals region, $R = 6 - 8$ a.u. A comprehensive study of the BMKP and BMKPE surfaces and how they compare with the Hinde PES for various geometries, H–H separations, and intermolecular distances is beyond the scope of this paper.

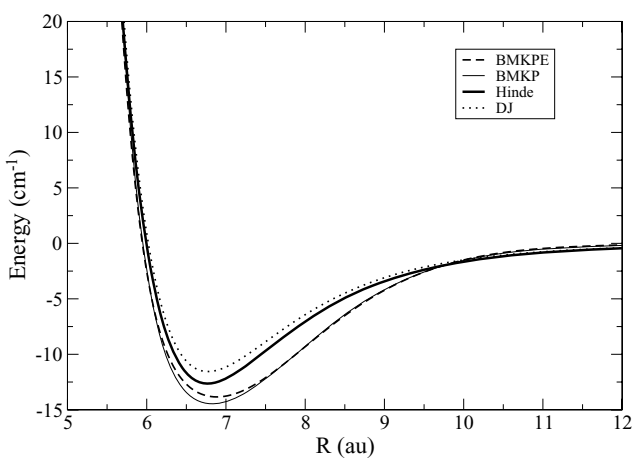

FIG. 7. Interaction potential, $U(r_1, r_2, R, \theta_1, \theta_2, \phi)$, obtained from BMKP (thin black curve), BMKPE (dashed curve), Hinde (thick black curve), and DJ (dotted curve) PESs as a function of R, computed for $r_1 = r_2 = 1.449$ a.u., $\theta_1 = \theta_2 = 90^\circ$, and $\phi = 0^\circ$.

B. Elastic scattering

Figure 8 provides a comparison of the elastic scattering cross section from the BMKP and Hinde PESs for H_2 $(v = 1, j = 0) + H_2(v = 0, j = 0)$ collisions as a function of the collision energy. It is seen that both PESs predict very similar results for collision energies spanning seven orders of magnitude, from the ultracold to thermal energy regime. Even the resonance features in the cross sections are quite well reproduced by the two PESs though their positions are slightly shifted. The results show that the isotropic part of the two PESs are similar and well characterized. Similar results for collisions involving ground state molecules on the Hinde and BMKP PESs and those of Lee *et al.* obtained using the rigid rotor (RR) DJ PES are shown in Fig. 9. It is seen that the Hinde and DJ PESs yield nearly identical results while

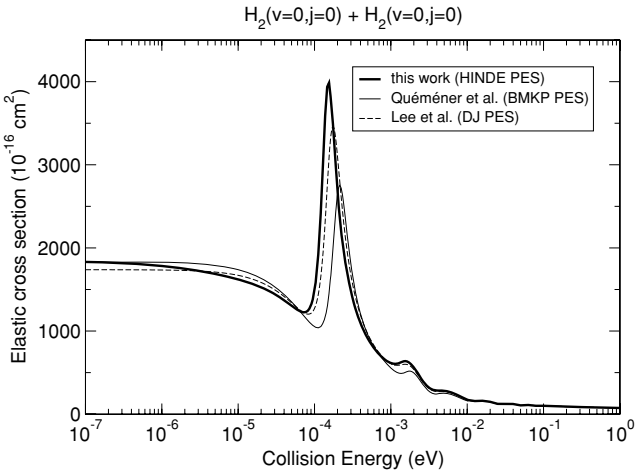

FIG. 9. Elastic cross sections as functions of the collision energy for $H_2(v = 0, j = 0) + H_2(v = 0, j = 0)$ collisions. The bold curve corresponds to the Hinde PES while the thin solid curve corresponds to the BMKP PES (taken from Ref. 41) and the thin dashed curve corresponds to the DJ PES (taken from Ref. 37).

the BMKP result shows discrepancies in the position and magnitude of the shape resonance located at about 10^{-4} eV. A comparison of elastic cross sections for $H_2(v = 0, j = 0) + H_2(v = 0, j = 0)$ collisions from the Hinde, BMKP, and DJ PESs with experimental data is given in Fig. 10. It shows that the Hinde and DJ PESs yield results in better agreement with experiment.

C. Rotational excitation

There have been several recent quantum studies of rotational excitation in collisions of two ground state H_2 molecules.[36,37,41,43,45,49,52] Earlier studies[36,37,52] have mostly used the rigid rotor approximation while recent studies using the BMKP PES by Otto *et al.*[45] and Quéméner and Balakrishnan[41] have used full-dimensional quantum calculations. Figure 11 shows cross sections for rotational excitations

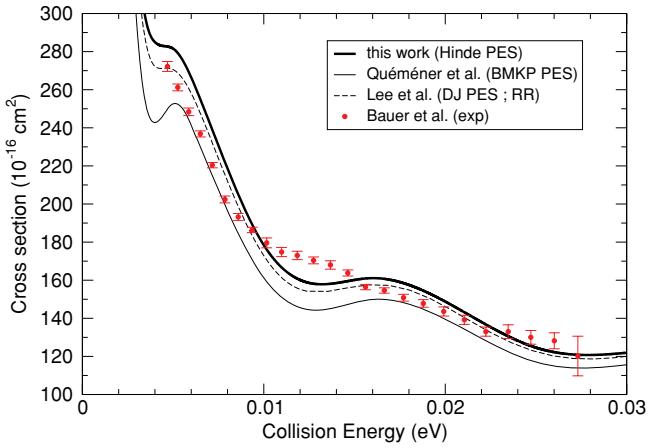

FIG. 10. Same as Fig. 9 but for a restricted range of collision energies for which experimental data are available. Experimental results of Bauer *et al.* (Ref. 65) are also shown. The experimental results have been multiplied by a factor of 2 to be consistent with the cross section formula adopted in this work.

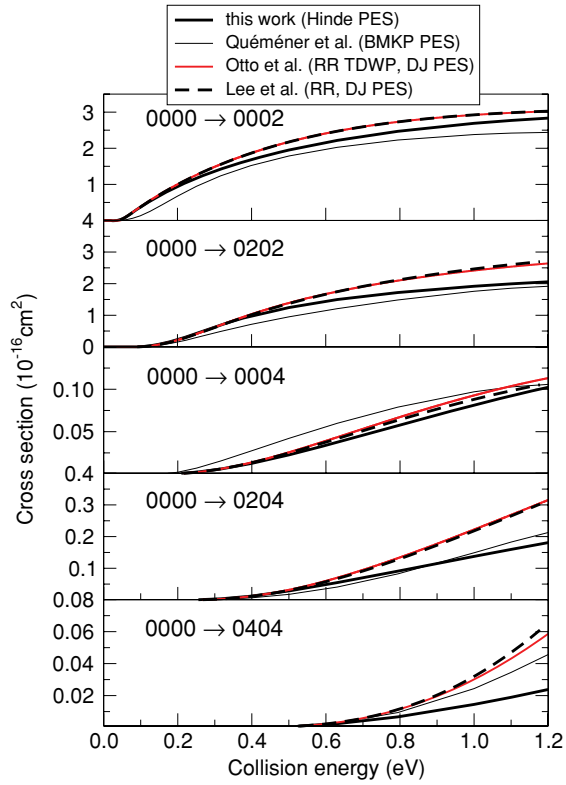

FIG. 11. State-to-state cross sections for rotational excitation in $H_2(v = 0, j = 0) + H_2(v = 0, j = 0)$ collisions as functions of the collision energy. The thick black curve corresponds to the Hinde PES while the thin black curve denotes the BMKP PES (taken from Ref. 41). The red and dashed curves, respectively, denote results obtained by Otto *et al.* (taken from Refs. 45 and 46) and Lee *et al.* (Ref. 37) using the DJ PES.

in collisions between two ground state *para*-H_2 molecules. Results for (0000) → (0002), (0004), (0204), and (0404) transitions from the present full-dimensional calculations using the Hinde surface and those of Quéméner and Balakrishnan[41] on the BMKP PES are compared with rigid rotor calculations of Otto *et al.*[46] and Lee *et al.*[37] using the DJ PES. (In our previous work[41] we had pointed out some discrepancy with the calculations of Otto *et al.*[45] The source of the discrepancy has now been identified[46] and the corrected results of Otto *et al.*[46] are shown in Fig. 11). The rigid rotor results are nearly identical for all transitions. It is seen that at low energies the results obtained using DJ and Hinde PESs agree quite well but discrepancies are observed at higher energies, particularly for (0202), (0204), and (0404) final CMSs. Overall, the BMKP results shows significant discrepancy with those computed using the DJ and Hinde PESs, particularly at low energies. As shown below, this has a significant effect on low temperature rate coefficients computed using the BMKP surface.

Figure 12 compares rate coefficients for (0000) → (0002) rotational excitation from full-dimensional calculations using the Hinde and BMKP PESs with the experimental results of Maté *et al.*[52] The BMKP results are taken from previous work of Quéméner and Balakrishnan.[41] It is seen that the results on the Hinde PES agree reasonably well with the experimental data while the BMKP surface predicts about a factor of 5–10 smaller rate coefficients. Previous cal-

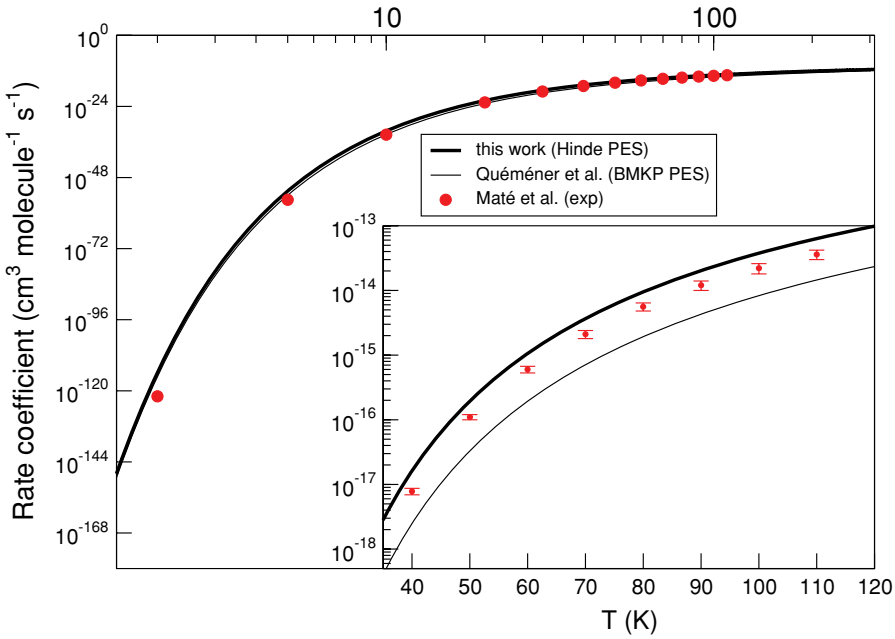

FIG. 12. Rate coefficient as a function of the temperature for $H_2(v = 0, j = 0) + H_2(v = 0, j = 0) \rightarrow H_2(v = 0, j = 2) + H_2(v = 0, j = 0)$ collisions. The bold curve corresponds to the Hinde PES while the thin solid curve corresponds to the BMKP PES (taken from Ref. 41). Experimental results of Maté *et al.* (Ref. 52) are also shown.

culations using the DJ PES have shown that it yields results in close agreement with experimental data for the $0 \rightarrow 2$ rotational excitation.[37] Thus, it appears that the BMKP PES needs some additional constraints on its angular dependence to yield reliable values of rotational and vibrational transition rate coefficients.

IV. CONCLUSION

We have presented cross sections and rate coefficients for rotational and vibrational transitions in collisions between two H_2 molecules. A full-dimensional quantum scattering method without any angular momentum decoupling approximation is used for the calculations. A recent six-dimensional potential energy surface for the H_2–H_2 system developed by Hinde[54] has been used in the calculations and comparisons are made with results obtained using the more widely used BMKP PES and its less anisotropic version referred to as the BMKPE PES.

The paper presents several important results on the H_2–H_2 system. First, it showed that a near-resonant energy transfer mechanism for vibrational relaxation identified in our previous study using the BMKP PES is also reproduced by the Hinde PES. The mechanism approximately conserves the internal energy and fully conserves the total internal rotational angular momentum of the two molecules. The present study shows that the mechanism is largely insensitive to the details of the interaction potential (including angular anisotropy) and may be a general phenomenon observed in other dimer systems. It also shows that in instances where the above mechanism is not involved, vibrational relaxation is largely driven by the angular anisotropy of the interaction potential.

Another key finding of our study is that the Hinde PES predicts rate coefficients for vibrational relaxation in $H_2(v = 1, j = 0) + H_2(v = 0, j = 0)$ collisions in close agreement with available experimental data. Interestingly, the vibrational relaxation rate coefficients obtained using the Hinde PES agree more closely with those derived from the less anisotropic BMKPE potential than with those derived from the full BMKP PES. The latter predicts vibrational relaxation rate coefficients that are an order of magnitude greater than experimental results as originally pointed out by Pogrebnya and Clary. The present study lends theoretical support to the argument that high-order angular anisotropic terms of the BMKP potential is responsible for the discrepantly large values of the relaxation rate coefficients using this PES.

Comparing the results obtained using the two full-dimensional PESs (Hinde and BMKP) with those derived from the rigid rotor DJ PES, we find that the agreement is substantially better between the Hinde and DJ results than between the BMKP and DJ results. Rate coefficients for the $0 \rightarrow 2$ rotational excitation computed using the Hinde PES is found to be in good agreement with experimental data. Overall, it appears that the Hinde and DJ PESs yield more reliable values of rotational transition rate coefficients. Based on the calculations presented here, we recommend the use of the newer Hinde PES for calculations of rotational and vibrational transitions in H_2–H_2 collisions, at least for vibrational quantum numbers $v < 2$. *Ab initio* calculations of the Hinde PES include only a limited range of H–H separations so its accuracy for higher vibrational levels is uncertain.

ACKNOWLEDGMENTS

This work was supported by NSF Grant Nos. PHY-0855470 (N.B.), ATM-0635715 (N.B.), PHY-0854838 (R.C.F.), and AST-0607733 (P.C.S.). Partial support from National Aeronautics and Space Administration under

Grant/Cooperative Agreement No. NNX08AE57A issued by the Nevada NASA EPSCoR program is also acknowledged. We thank F. Otto for providing us their theoretical results and R. Krems for useful discussions and initial collaboration on this project.

[1]N. Balakrishnan, R. C. Forrey, and A. Dalgarno, Phys. Rev. Lett. **80**, 3224 (1998).
[2]R. V. Krems, Int. Rev. Phys. Chem. **24**, 99 (2005).
[3]P. F. Weck and N. Balakrishnan, Int. Rev. Phys. Chem. **25**, 283 (2006).
[4]J. M. Hutson and P. Soldán, Int. Rev. Phys. Chem. **25**, 497 (2006).
[5]E. Bodo and F. A. Gianturco, Int. Rev. Phys. Chem. **25**, 313 (2006).
[6]G. Quéméner, N. Balakrishnan, and A. Dalgarno, in *Cold Molecules: Theory, Experiment, Applications*, edited by R. Krems, W. C. Stwalley, and B. Friedrich (CRC Press, Boca Raton, 2009), pp. 69–124.
[7]D. Herschbach, Faraday Discuss. **142**, 9 (2009).
[8]D. W. Chandler, J. Chem. Phys. **132**, 110901 (2010).
[9]E. P. Wigner, Phys. Rev. **73**, 1002 (1948).
[10]P. Soldán, M. T. Cvitaš, J. M. Hutson, P. Honvault, and J.-M. Launay, Phys. Rev. Lett. **89**, 153201 (2002).
[11]G. Quéméner, P. Honvault, and J.-M. Launay, Eur. Phys. J. D **30**, 201 (2004).
[12]G. Quéméner, P. Honvault, J.-M. Launay, P. Soldán, D. E. Potter, and J. M. Hutson, Phys. Rev. A **71**, 032722 (2005).
[13]M. T. Cvitaš, P. Soldán, J. M. Hutson, P. Honvault, and J.-M. Launay, Phys. Rev. Lett. **94**, 033201 (2005).
[14]M. T. Cvitaš, P. Soldán, J. M. Hutson, P. Honvault, and J.-M. Launay, Phys. Rev. Lett. **94**, 200402 (2005).
[15]G. Quéméner, N. Balakrishnan, and B. K. Kendrick, Phys. Rev. A **79**, 022703 (2009).
[16]G. Quéméner, J.-M. Launay, and P. Honvault, Phys. Rev. A **75**, 050701(R) (2007).
[17]N. Balakrishnan and A. Dalgarno, Chem. Phys. Lett. **341**, 652 (2001).
[18]E. Bodo, F. A. Gianturco, and A. Dalgarno, J. Chem. Phys. **116**, 9222 (2002).
[19]N. Balakrishnan and A. Dalgarno, J. Phys. Chem. A **107**, 7101 (2003).
[20]E. Bodo, F. A. Gianturco, N. Balakrishnan, and A. Dalgarno, J. Phys. B **37**, 3641 (2004).
[21]N. Balakrishnan, J. Chem. Phys. **121**, 5563 (2004).
[22]P. F. Weck and N. Balakrishnan, Eur. Phys. J. D **31**, 417 (2004).
[23]P. F. Weck and N. Balakrishnan, J. Chem. Phys. **122**, 154309 (2005).
[24]P. F. Weck and N. Balakrishnan, J. Chem. Phys. **122**, 234310 (2005).
[25]P. F. Weck and N. Balakrishnan, J. Chem. Phys. **123**, 144308 (2005).
[26]P. F. Weck, N. Balakrishnan, J. Brandao, C. Rosa, and W. Wang, J. Chem. Phys. **124**, 074308 (2006).
[27]G. Quéméner and N. Balakrishnan, J. Chem. Phys. **128**, 224304 (2008).
[28]C. Ticknor and J. L. Bohn, Phys. Rev. A **71**, 022709 (2005).
[29]R. V. Krems, Phys. Chem. Chem. Phys. **10**, 4079 (2008).
[30]T. V. Tscherbul, J. Chem. Phys. **128**, 244305 (2008).
[31]T. V. Tscherbul and R. V. Krems, J. Chem. Phys. **129**, 034112 (2008).
[32]G. Quéméner and J. L. Bohn, Phys. Rev A **81**, 022702 (2010).
[33]G. Quéméner and J. L. Bohn, Phys. Rev. A **81**, 060701(R) (2010).
[34]S. Ospelkaus, K.-K. Ni, D. Wang, M. H. G. de Miranda, B. Neyenhuis, G. Quéméner, P. S. Julienne, J. L. Bohn, D. S. Jin, and J. Ye, Science **327**, 853 (2010).
[35]K.-K. Ni, S. Ospelkaus, D. Wang, G. Quéméner, B. Neyenhuis, M. H. G. de Miranda, J. L. Bohn, J. Ye, and D. S. Jin, Nature (London) **464**, 1324 (2010).
[36]R. C. Forrey, Phys. Rev. A **63**, 051403 (2001).
[37]T.-G. Lee, N. Balakrishnan, R. C. Forrey, P. C. Stancil, D. R. Schultz, and G. J. Ferland, J. Chem. Phys. **125**, 114302 (2006).
[38]D. R. Flower and E. Roueff, J. Phys. B **31**, 2935 (1998).
[39]D. R. Flower and E. Roueff, J. Phys. B **32**, 3399 (1999).
[40]G. Quéméner, N. Balakrishnan, and R. V. Krems, Phys. Rev. A **77**, 030704(R) (2008).
[41]G. Quéméner and N. Balakrishnan, J. Chem. Phys. **130**, 114303 (2009).
[42]S. K. Pogrebnya and D. C. Clary, Chem. Phys. Lett. **363**, 523 (2002).
[43]S. Y. Lin and H. Guo, J. Chem. Phys. **117**, 5183 (2002).
[44]S. Y. Lin and H. Guo, J. Phys. Chem. A **107**, 7197 (2003).
[45]F. Otto, F. Gatti, and H.-D. Meyer, J. Chem. Phys. **128**, 064305 (2008).
[46]F. Otto, F. Gatti, and H.-D. Meyer, J. Chem. Phys. **131**, 049901 (2009).
[47]J. Le Bourlot, G. Pineau de Forêts, and D. R. Flower, Mon. Not. R. Astron. Soc. **305**, 802 (1999).
[48]*Molecular Hydrogen in Space*, edited by F. Combes and G. Pineau des Forêts (Cambridge University Press, Cambridge, UK, 2000).
[49]T.-G. Lee, N. Balakrishnan, R. C. Forrey, P. C. Stancil, G. Shaw, D. R. Schultz, and G. J. Ferland, Astrophys. J. **689**, 1105 (2008).
[50]A. I. Boothroyd, P. G. Martin, W. J. Keogh, and M. J. Peterson, J. Chem. Phys. **116**, 666 (2002).
[51]P. Diep and J. K. Johnson, J. Chem. Phys. **112**, 4465 (2000).
[52]B. Maté, F. Thibault, G. Tejeda, J. M. Fernández, and S. Montero, J. Chem. Phys. **122**, 064313 (2005).
[53]K. Patkowski, W. Cencek, P. Jankowski, K. Szalewicz, J. B. Mehl, G. Garberoglio, and A. H. Harvey, J. Chem. Phys. **129**, 094304 (2008).
[54]R. J. Hinde, J. Chem. Phys. **128**, 154308 (2008).
[55]K. Takayanagi, Adv. At. Mol. Phys. **1**, 149 (1965).
[56]S. Green, J. Chem. Phys. **62**, 2271 (1975).
[57]M. H. Alexander and A. E. DePristo, J. Chem. Phys. **66**, 2166 (1977).
[58]G. Zarur and H. Rabitz, J. Chem. Phys. **60**, 2057 (1974).
[59]A. M. Arthurs and A. Dalgarno, Proc. R. Soc. London, Ser. A **256**, 540 (1960).
[60]R. V. Krems, Two BC–quantum scattering program, University of British Columbia, Vancouver, Canada, 2006.
[61]B. R. Johnson, J. Comp. Phys. **13**, 445 (1973).
[62]D. E. Manolopoulos, J. Chem. Phys. **85**, 6425 (1986).
[63]A. J. McCaffery, Phys. Chem. Chem. Phys. **6**, 1637 (2004).
[64]M.-M. Audibert, R. Vilaseca, J. Lukasik, and J. Ducuing, Chem. Phys. Lett. **31**, 232 (1975).
[65]W. Bauer, B. Lantzsch, J. P. Toennies, and K. Walaschewski, Chem. Phys. **17**, 19 (1976).
[66]J. Schaefer and W. E. Köhler, Z. Phys. D: At., Mol. Clusters **13**, 217 (1989).
[67]D. W. Schwenke, J. Chem. Phys. **89**, 2076 (1988).